Journal of the Korean Society of Oceanography
Vol. 38, No. 4, pp. 157 — 165 December 2003

Estimation of Sedimentation and Particle Mixing Rates in Ulleung Basin of the East Sea (Sea of Japan) Using ^{7}Be, ^{234}Th, ^{210}Pb and ^{137}Cs

KEE HYUN KIM* AND NAM JOON PARK
Department of Oceanography and Ocean Environmental Sciences, Chungnam National University, Daejeon 305-764, Korea

In order to understand the characteristics of sedimentary environments in Ulleung Basin of the East Sea (Sea of Japan), three sediment cores were taken with a box corer during R/V Tamyang cruise in October 1999. Activities of ^{7}Be, ^{210}Pb, ^{226}Ra, ^{234}Th, ^{238}U and ^{137}Cs in sediment samples were determined by non-destructive gamma-ray spectrometry. Rates of sedimentation and particle mixing were estimated by best fitting an advection-diffusion particle mixing model to the data of ^{7}Be, ^{234}Th and ^{210}Pb. Estimated sedimentation rates were 0.06–0.08 cm/yr and particle mixing rates were 0.13–0.65 cm^2/yr. The use of multiple tracers in our study prevented us from probable up to 38% overestimation of sedimentation rates.

Key words: Sedimentation Rate, Particle Mixing Rate, ^{7}Be, ^{210}Pb, ^{234}Th

INTRODUCTION

Three naturally occurring radionuclides, ^{7}Be, ^{234}Th and ^{210}Pb, have been used extensively to study marine sedimentation. Beryllium-7 ($t_{1/2}$=53.3d) is produced by spallation processes in the upper layer of the Earth's atmosphere. Because ^{7}Be is produced in enough abundance to be readily detectible in natural samples of water and sediments (Dibb and Rice, 1989), ^{7}Be has attracted considerable attention as a tracer of short-term processes in aquatic systems. Recent works have demonstrated its applicability in coastal and estuarine waters (Aaboe *et al.*, 1981; Dibb and Rice, 1989; Baskaran *et al.*, 1997; Cochran *et al.*, 1998; Gerino *et al.*, 1998; Feng *et al.*, 1999). ^{7}Be has also been used in the study of mixing in the top few centimeters of sediment (Krishnaswami *et al.*, 1980; Casey *et al.*, 1986).

Radiogenic ^{234}Th is produced by alpha decay of ^{238}U dissolved in seawater. On its production, ^{234}Th is rapidly adsorbed onto particles and removed to sediments. Its half-life is so short (24.1d) that it can be used to study sediment mixing processes occurring on time scales of approximately 100 days (Aller *et al.*, 1980). Excess ^{234}Th has been used as an excellent tracer for biogenic and physical reworking of particles in near shore sediments (Aller and Cochran, 1976; 1984; Kim and Burnett, 1988; Feng *et al.*, 1999).

*Corresponding author: khkim@cnu.ac.kr

In the coastal seas, most of excess ^{210}Pb originates from radioactive decay of ^{222}Rn in the atmosphere and the subsequent precipitation of ^{210}Pb to the sea (Goldberg *et al.*, 1962). In addition to the atmospheric influx, dissolved ^{226}Ra in seawater is an additional source of the excess ^{210}Pb in sediments. With a half-life of 22.3 years, ^{210}Pb has been proved to be an important nuclide for the study of sedimentary processes. Because of its relatively longer half-life than those of ^{7}Be and ^{234}Th, ^{210}Pb allows measurements of sediment mixing rate occurring on time scales of up to 100 years in estuary, fjord, continental margin and shelf (Nittrourer *et al.*, 1983; Kim and Burnett, 1988; Hong *et al.*, 1997; Moon, 1999; Jaeger and Nittrouer, 1999). Moreover, ^{210}Pb has been used to study rates of particle mixing in deep-sea sediments (Nozaki *et al.*, 1977; Hong *et al.*, 1997; Moon, 1999).

Estimation of sedimentation rate is the primary concern in studying sedimentary process. The sedimentation rates could be estimated from the activity gradient of vertical distribution of radionuclides. Intense physical and biological activity at the sediment-water interface can cause mixing and displacement of surface sediments. Particle mixing can influence the distribution of chemical species in the interfacial zone and smear the stratigraphic record of sediments (Krishnaswami *et al.*, 1980). Particle mixing flattens the activity gradient of radionuclides in sediments, resulting in overestimation of sedimentation rates. Therefore, for the

accurate estimate of sedimentation rates, both rates of sedimentation and particle mixing should be considered simultaneously.

We present here the results from our recent study on the radionuclides in 3 sediment cores from the East Sea. In this study, we considered sedimentation and particle mixing simultaneously. Moreover, we employed 4 radionuclides, ^{7}Be, ^{234}Th, ^{210}Pb and ^{137}Cs, in order to pinpoint both rates and to cross-check the results among the different tracers.

MATERIALS AND METHODS

Study area

The East Sea is a typical inactive back-arc basin with an average water depth of 1,350 m and is characterized by a semi-enclosed marginal sea with four shallow straits: Tsugaru (130 m deep), Korea (Tsushima) (130 m deep), Soya (55 m deep) and Tatarshiya (15 m deep) Straits (Hyun *et al.*, 1998).

There are three deep basins in the East Sea: the Japan, Yamato and Ulleung Basins. These basins are separated by ridges such as the Korea Plateau, Oki Bank, Yamato Ridge and Kita-Yamato Ridge. The general bathymetry of Ulleung Basin is characterized by a northeastward U-shaped gentle slope. The basin extends northeastward through gap between Ulleung and Tok Islands, forming a narrow and long inter-basin plain. The floor of Ulleung Basin is generally flat and progressively deeper northward, connected to Japan Basin by Ulleung Interplain Channel (Chough *et al.*, 1985), which is approximately 7 km wide and 35 m deep. It is erosional in origin and undercuts the turbidite sequence, formed most likely by strong bottom currents flowing through the gap (Chough, 1984).

On board works

Sediment samples were taken with a box corer during R/V Tamyang cruise in October 1999. The location (by GPS) and water depth (by echo sounder) of the coring sites are presented in Fig. 1 and Table 1. Immediately after the box corer was retrieved on board, subcores were taken by inserting acrylic tubes (diameter 10 cm) by hand into the sediment without disturbing the sediment surface.

Analytical methods

Subcores were carefully sectioned into 1-cm interval in the laboratory immediately after returning from the cruise. Sectioned samples were dried at 80°C in an oven for 48 hours, ground to powder, loaded into plastic counting vials with caps, weighed and sealed air-tightly with glue and para-film. Water content and dry bulk density (Lee and Chough, 1987) were measured in the laboratory to understand physical properties of sediments.

Activities of ^{7}Be, ^{210}Pb, ^{226}Ra, ^{234}Th, ^{238}U and ^{137}Cs in sediment samples were determined by non-destructive gamma-ray spectrometry following the proce-

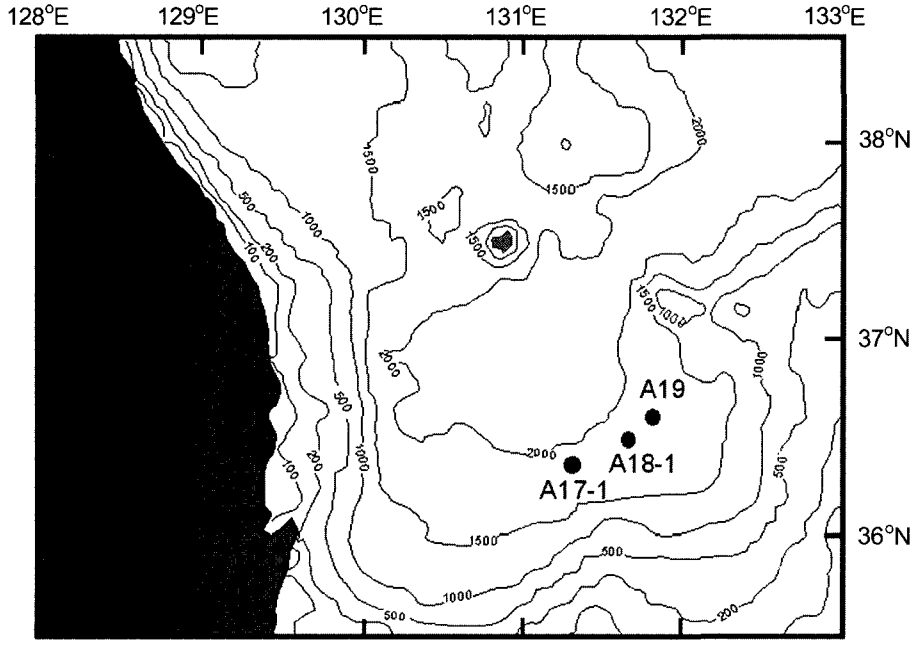

Fig. 1. Map showing the location of sediment cores collected by box-corer in Ulleung Basin of the East Sea. Unit for the depth contour is in meters (m).

Table 1. Location data of the coring sites in Ulleung Basin of the East Sea.

Station	Water depth (m)	Location		Date	Remark
		Latitude (°N)	Longitude ((°N)E)		
A17-1	1,927	36°18.83′	131°18.88′	99.10.11	Box core
A18-1	1,867	36°29.51′	131°39.63′	99.10.12	"
A19	1,827	36°34.44′	131°50.55′	99.10.12	"

dures described by Kim and Burnett (1983) utilizing a well-type intrinsic germanium detector (WIGe: Canberra Model GCW 2021). All the samples were counted twice in approximately 3 month intervals: the first counting for ^{7}Be, total ^{234}Th, ^{210}Pb and ^{137}Cs; and the second counting for ^{226}Ra and ^{238}U via the ^{234}Th peak. The activity of ^{7}Be was determined by a photopeak at 477.6 keV, ^{210}Pb at 46.5 keV and ^{137}Cs at 661.6 keV. ^{226}Ra activity was determined by taking the average activities obtained by three photopeaks: ^{214}Pb at 295 and 352 keV and ^{214}Bi at 609 keV. ^{234}Th was determined by its own peak at 63 keV. The activities of ^{234}Th and ^{238}U were calculated by the standard radioactivity growth-decay equation (Bateman, 1910) and using data from the first and the second countings.

The efficiency of the WIGe detector was calibrated with radioactive standard materials supplied by the Environmental Monitoring Systems Laboratory of the Environmental Protection Agency (EPA) and the National Bureau of Standards (NBS). The efficiency of ^{7}Be was calculated from the experimental equation of full-energy peak efficiency curve. Self absorption correction was not considered because the matrices of standards and samples were similar.

All activities of ^{7}Be, $^{234}Th_{xs}$ ($=^{234}Th_{total}-^{238}U$) and $^{210}Pb_{xs}$ ($=^{210}Pb_{total}-^{226}Ra$) were corrected for decay since the time of coring and for weight of sea salt in sediment. Salt-corrected activities are calculated by the following Eq. (1):

$$A = \frac{a}{m-\left\{\dfrac{m\cdot W_D\cdot h}{10^3(100-W_D)+W_D\cdot h}\right\}} \quad (1)$$

where: A=corrected activity for sea salt (mBq/g); a= activity (mBq/g); m=dry sediment weight (g); W_D= water content of sediment (%); h=salinity (‰). The factors of salt-correction were in the range of 0.36-0.92, smaller at the bottom of the core and greater at the top.

Mixing model

Processes affecting the vertical profiles of radionuclides in sediment column include particle mixing, sedimentation and radioactive decay. In this study, one-dimensional advection-diffusion particle mixing model was used to estimate the rates of sedimentation and particle mixing. The one-dimensional model has been widely used in most previous studies on marine sediments (Goldberg and Koide, 1962; DeMaster and Cochran, 1982; Aller and DeMaster, 1984; Cochran, 1995; Jaeger and Nittrouer, 1999).

The model equation is:

$$\frac{dC}{dt} = D\frac{\partial^2 C}{\partial z^2} - S\frac{\partial C}{\partial z} - \lambda C \quad (2)$$

where z=depth below the sediment surface (cm); C=the excess activity (dpm/g); λ=the decay constant of the radionuclide (yr^{-1}); D=the particle mixing coefficient (cm^2/yr); S=sedimentation rate (cm/yr).

At steady-state (dC/dt=0), general solution of the Eq. (2) is:

$$C = P\exp(Az) + Q\exp(Bz) \quad (3)$$

Where,

$$A = S + (\sqrt{S^2+4\lambda D})/2D$$

$$B = S - (\sqrt{S^2+4\lambda D})/2D$$

and P and Q are constants.

The two boundary conditions considered are: $C=C_0$ at z=0; and $C\rightarrow 0$ at $z\rightarrow\infty$.

Solving Eq. (3) with the boundary conditions yields Eqs. (4) and (5):

$$C_0 = P + Q \quad (4)$$

$$P\exp(Bz) = 0 \quad (5)$$

$$C = C_0\exp\left[\left(\frac{S-\sqrt{S^2+4\lambda D}}{2D}\right)z\right] \quad (6)$$

$$\ln C = \ln C_0 + \left[\frac{S-\sqrt{S^2+4\lambda D}}{2D}\right]z \quad (7)$$

RESULTS AND DISCUSSION

Physical properties

Water contents of all cores decrease gradually with depth and vary from 76% to 97% in the 3 cores. On the other hand, dry bulk densities increase with depth, in the range of 0.74–0.87 g/cm^3 (Table 2).

Distribution of ^{7}Be, ^{234}Th and ^{210}Pb

Table 2 shows the results of gamma spectroscopic analysis. The activities of the ^{7}Be, ^{234}Th$_{xs}$, ^{210}Pb$_{xs}$, ^{238}U and ^{226}Ra are plotted as a function of depth (Figs. 2, 3 and 4).

Penetration depth of the three nuclides for each cores were 6.5–7.5 cm for ^{7}Be, 5.5–7.5 cm for ^{234}Th$_{xs}$, and 11.5–15.5 cm for ^{210}Pb$_{xs}$ (Table 3). The penetration depths of three nuclides for each core are different because the chemistry and half-lives of three nuclides are different. Because of their shorter half-lives than ^{210}Pb, penetration of ^{7}Be and ^{234}Th are appeared be confined to top few centimeters of the cores (DeMaster and Cochran, 1982; Feng *et al.*, 1999).

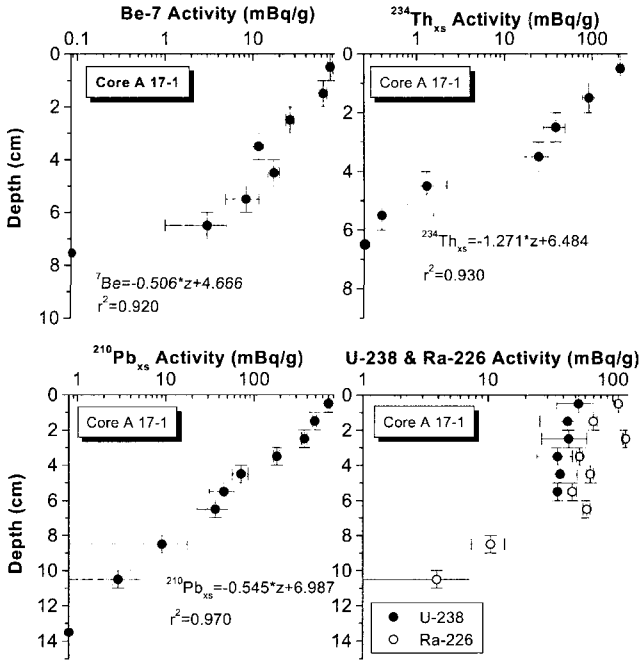

Fig. 2. Vertical profiles of ^{7}Be, ^{234}Th$_{xs}$, ^{210}Pb$_{xs}$, ^{238}U and ^{226}Ra activities in core A17-1. Least-square best-fit lines were drawn to the semi-logarithmic plots.

Table 2. Physical properties and radiochemical data for A17-1, A18-1 and A19 cores from Ulleung Basin of the East Sea.

Station	Depth (cm)	Water content (%)	Dry bulk density (g/cm^3)	^{7}Be (mBq/g)	^{234}Th$_{xs}$* (mBq/g)	^{210}Pb$_{xs}$† (mBq/g)	^{226}Ra (mBq/g)	^{238}U (mBq/g)	^{137}Cs (mBq/g)
A17-1	0–1	95.01	0.75	75.7±5.2	209±14	701±29	110.3±5.2	53±17	13.4±2.2
	1–2	91.45	0.77	63.2±6.3	91±15	490±25	69.71±4.6	43±17	16.0±1.8
	2–3	89.42	0.79	26.4±2.7	38±11	374±25	125.8±5.6	44±17	18.7±1.3
	3–4	87.39	0.80	11.6±1.6	24.3±7.4	182±14	54.1±3.2	36±12	6.0±1.0
	4–5	82.82	0.83	17.3±2.5	1.27±0.90	72±15	65.9±3.9	38±14	5.6±1.1
	5–6	85.36	0.81	8.3±3.4	0.4±1.2	46±15	47.3±4.0	36±15	3.5±1.2
	6–7	77.23	0.87	3.0±2.0	–	37±14	61.8±4.0	–	1.7±1.3
A18-1	0–1	94.50	0.76	80.3±6.6	183±15	533±24	74.2±4.1	40±14	14.9±1.8
	1–2	96.03	0.75	51.2±4.8	98±13	477±18	69.3±3.5	52±13	16.2±2.1
	2–3	97.55	0.74	74±10	137±28	450±27	85.6±5.8	52±22	20.4±3.4
	3–4	89.42	0.79	20.3±2.9	50.1±9.1	188±11	47.7±2.4	23.4±8.5	28.3±3.7
	4–5	88.40	0.79	24.9±3.6	28±11	205±13	33.9±2.8	23±11	6.7±1.4
	5–6	84.85	0.82	18.9±4.2	21±11	155±12	50.0±2.9	19±11	2.4±1.2
	6–7	81.80	0.84	7.0±2.1	7.0±7.2	70.2±7.9	37.0±2.0	14.0±7.2	1.41±0.60
	7–8	76.72	0.87	1.8±1.8	3.4±1.8	34.8±8.9	46.1±2.5	13.0±8.9	–
A19	0–1	97.04	0.74	93.7±6.7	291±14	788±19	92.3±2.3	54±18	11.9±2.5
	1–2	95.52	0.75	61.7±6.8	148±15	524±20	69.5±2.0	48±19	13.4±2.6
	2–3	96.03	0.75	45.9±7.2	78±14	437±23	78.2±3.2	61±21	15.5±1.7
	3–4	91.45	0.77	20.7±2.7	28±11	68.8±7.3	50.9±1.4	38±12	4.2±2.3
	4–5	93.49	0.76	21.0±3.2	61±12	74±10	49.9±1.6	48±18	4.4±1.1
	5–6	87.39	0.80	8.4±2.7	27.3±8.9	45.8±7.8	48.7±1.7	33±14	1.7±1.1
	6–7	82.82	0.83	2.9±1.6	7.5±6.6	28.2±5.9	49.4±1.2	9.0±1.7	–

*^{234}Th$_{xs}$ = ^{234}Th$_{1st}$ – ^{234}Th$_{2nd}$, ^{234}Th$_{2nd}$ = ^{238}U; †^{210}Pb$_{xs}$ = ^{210}Pb$_{total}$ – ^{226}Ra; Water content are based on dry sediment weight.

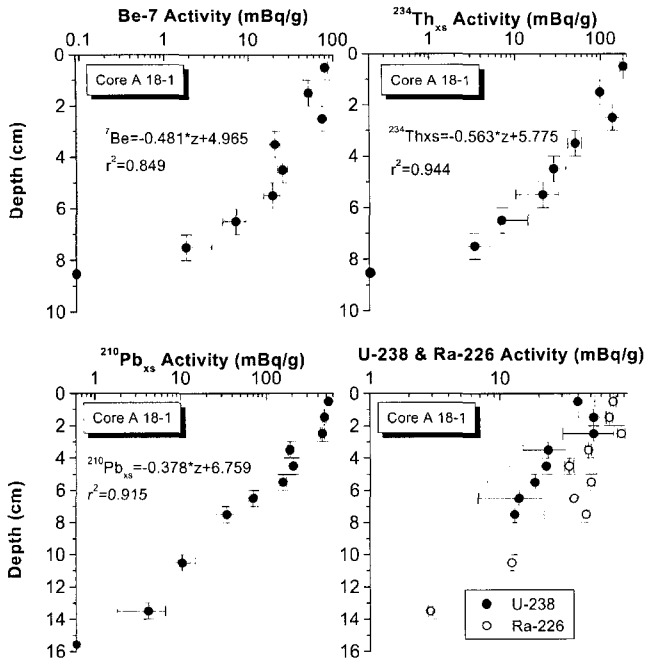

Fig. 3. Vertical profiles of ^{7}Be, $^{234}Th_{xs}$, $^{210}Pb_{xs}$, ^{238}U and ^{226}Ra activities in core A18-1. Least-square best-fit lines were drawn to the semi-logarithmic plots.

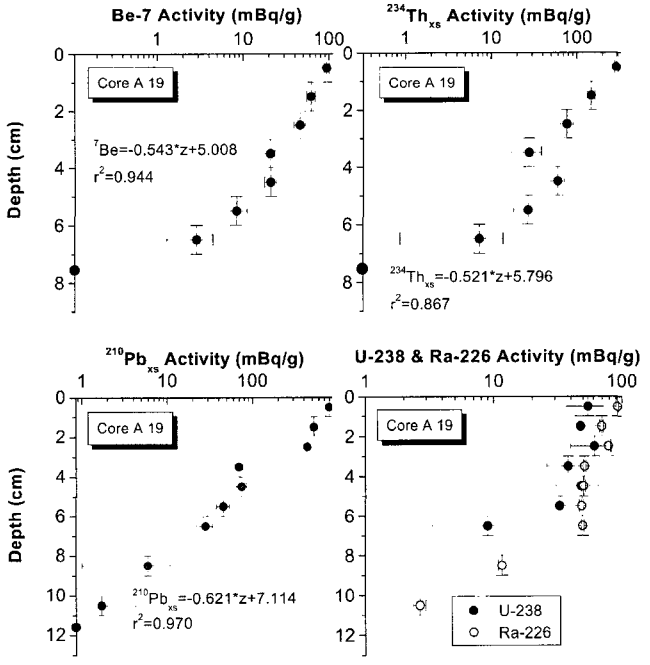

Fig. 4. Vertical profiles of ^{7}Be, $^{234}Th_{xs}$, $^{210}Pb_{xs}$, ^{238}U and ^{226}Ra activities in core A19. Least-square best-fit lines were drawn to the semi-logarithmic plots.

Rates of particle mixing and sedimentation

Since half-lives of ^{7}Be and ^{234}Th are very short, sedimentation rates can not be estimated from these nuclides but particle mixing rates can be obtained. Assuming S^2 is negligible compared to $4\lambda D$ (i.e., $4\lambda D >> S^2$), Eq. (7) can be simplified to:

$$\ln C = \ln C_0 - \left[\sqrt{\frac{\lambda}{D}}\right] z \qquad (8)$$

Thus, the slopes of the regression lines ($\sqrt{\lambda/D}$) fitted to ^{7}Be and ^{234}Th profiles yield two D values for each core, D_{Be} and D_{Th}, respectively. It has been reported that the D values derived from ^{234}Th and ^{210}Pb were different in same cores, due to the particle selective mixing of benthic organisms (Krishnaswami *et al.*, 1980; Feng *et al.*, 1999). We presume the same mechanism operated in our cores, therefore, the different D values were derived from ^{7}Be and ^{234}Th. Estimated particle mixing rates in Ulleung Basin were in the range from 0.13 cm^2/yr to 0.65 cm^2/yr (Table 4). These values are similar to those of the deep Pacific sediments below the oligotrophic surface waters with low productivity (Table 5). Mixing rates of the deep

Table 3. Core-top activities (C_0) where depth is zero (z=0) and penetration depths (L) for each nuclides. Core-top activities were calculated from the intercept values of least-square regression equations.

Station No.	^{7}Be		$^{234}Th_{xs}$		$^{210}Pb_{xs}$		Remark
	C_0 (mBq/g)	L (cm)	C_0 (mBq/g)	L (cm)	C_0 (mBq/g)	L (cm)	
A17-1	106.3	6.5	654.6	5.5	1082.3	12.5	Core-top preserved
A18-1	143.3	7.5	322.1	7.5	861.8	15.5	"
A19	149.6	7.5	329.0	7.5	1140.3	11.5	"

Table 4. Assuming S^2 is negligible compared to $4\lambda D$, particle mixing rates were obtained by ^{7}Be (D_{Be}) and $^{234}Th_{xs}$ (D_{Th}), respectively. D_{mean} values are averages of D_{Be} and D_{Th}. See details in text.

Station No.	D_{Be} (cm^2/yr)	D_{Th} (cm^2/yr)	D_{mean} (cm^2/yr)	S (cm/yr)
A17-1	0.16	0.33	0.25	0.06
A18-1	0.19	0.65	0.42	0.08
A19	0.13	0.28	0.21	0.07

Table 5. Rates of sedimentation and particle mixing ^{7}Be, ^{234}Th and ^{210}Pb in Ulleung Basin of the East Sea. Bold numbers indicate the sedimentation rates estimated with considering particle mixing and italics without considering particle mixing.

Station No.	Sedimentation rate (cm/yr)	Particle mixing rate (cm^2/yr)	Reference
A17-1	**0.06±0.01**	0.16–0.33	This study
A18-1	**0.08±0.02**	0.19–0.65	"
A19	**0.07±0.02**	0.13–0.28	"
East Sea	**0.02–0.15**	0.09–0.81	Moon, 1999
East Sea	*0.04–0.22*		Hong et al., 1997
East Sea	*0.07–0.30*		MOST, 1995
Antarctic		0.04–0.16	DeMaster et al., 1982
Deep Pacific		0.22–0.40	DeMaster et al., 1982
Deep Pacific		0.08–0.77	Cochran, 1985
Upwelling sea, Peru Margin		0.19–4.6	Kim and Burnett, 1988

Pacific sediments were 0.22–0.40 cm^2/yr (DeMaster *et al.*, 1982) and 0.08–0.77 cm^2/yr (Cochran, 1985). Also, these results are similar to those of previous study in the East Sea (Moon, 1999). Mixing rates in Ulleung Basin were, however, estimated to be lower than those obtained from the Peru upwelling sea (Kim and Burnett, 1988).

Using the D_{mean} value, which is the mean of D_{Be} and D_{Th}, we could estimate S for each core from equation (7) best-fitted to $^{210}Pb_{ex}$ profiles. Sedimentation rates are 0.06±0.01 cm/yr for A17-1, 0.08±0.02 cm/yr for A18-1, and 0.07±0.02 cm/yr for A19. These sedimentation rates of 3 cores could be same due to overlapped error bars.

Subsurface maximums of ^{137}Cs

Activities of ^{137}Cs in 3 cores are plotted in Fig. 5, clearly showing subsurface maximums. Core A19 displayed a ^{137}Cs peak at the sediment depth of 2.5 cm, corresponding to the deposition year of 1963 on the basis of ^{210}Pb-derived sedimentation rate of 0.07 cm/yr. Maximum activities of ^{137}Cs occurred at depth interval of 2–3 cm in core A17-1 and 3–4 cm in core A18-1. These intervals still envelop the sediment depths deposited in early 1960s. This trend of ^{137}Cs peak depth can be explained by the well-documented global input function of ^{137}Cs (Jaakola *et al.*, 1983; Miller and Heit, 1986). We presume our estimates of sedimentation rates in this area to be close to real values.

Spatial distribution of sedimentation rates

Figure 6 shows the spatial distribution of sedimentation rates in Ulleung Basin. The results of this study are similar to those of previous studies in the East Sea (Moon, 1999; Hong *et al.*, 1997). However,

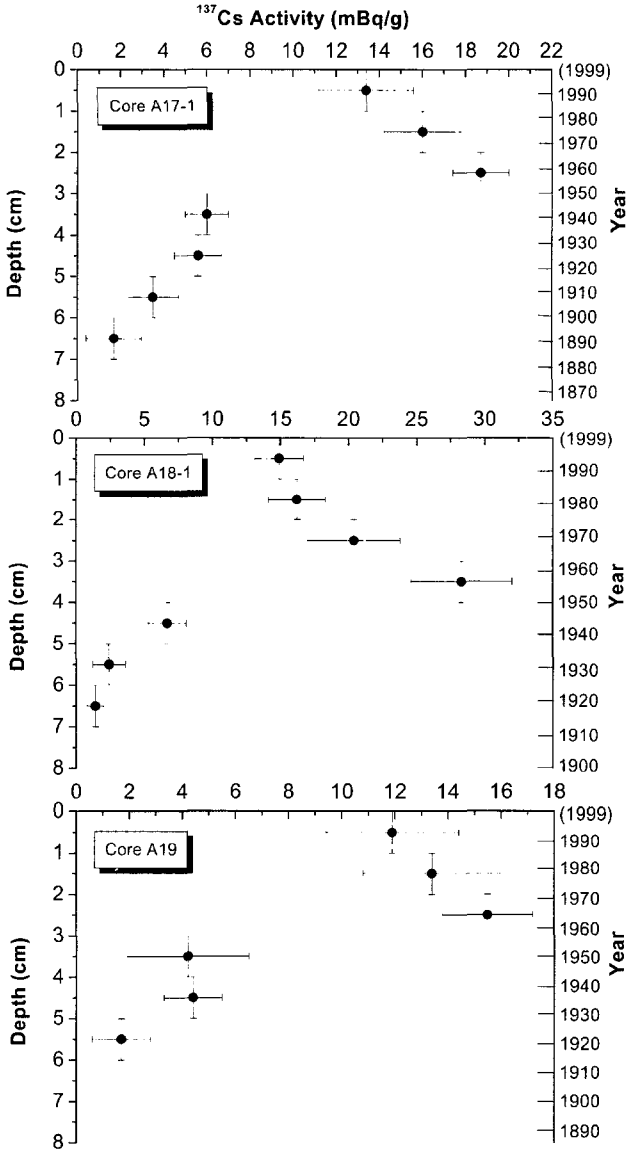

Fig. 5. Vertical profiles of ^{137}Cs activity in sediment of cores A17-1, A18-1 and A19. Years of sediment deposition were assigned based on the mixing-considered ^{210}Pb-derived sedimentation rates.

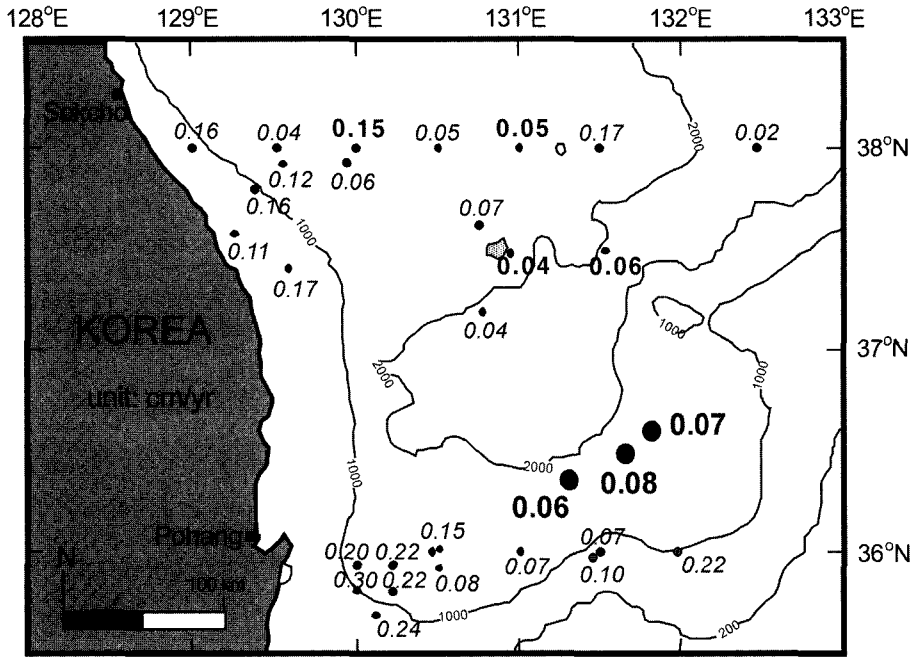

Fig. 6. Distribution of sedimentation rates (S, cm/yr) in Ulleung Basin of the East Sea. Bold numbers indicate S values estimated with mixing considered, while italic numbers without mixing considered.

Table 6. Comparison of estimated sedimentation rates between two cases, particle mixing ignored and mixing considered. D_{mean} values were used in calculation of S.

Station No.	Sedimentation rate (cm/yr)		Difference (%)
	Mixing ignored (D=0)	Mixing considered (D>0)	
A17-1	0.07±0.03	0.06±0.01	17
A18-1	0.11±0.03	0.08±0.02	38
A19	0.08±0.04	0.07±0.02	14

the rates reported by Moon (1999) were estimated with considering particle mixing. On the other hand, all the other estimates were obtained without considering mixing, thus presumably overestimation.

Sensitivity of the rate estimation

We have found that estimated sedimentation rates were very sensitive to particle mixing. Table 6 shows the result of comparison between the two cases: particle mixing ignored and mixing considered (D_{mean} values were used in calculation of S). When particle mixing rate was not considered, the resulting sedimentation rates could be overestimated up to 38%. Therefore, we presume that reliability of sedimentation rates would be much more improved by considering particle mixing together.

Inventory and flux

Marine sediment is a reservoir of natural radionuclides which were supplied from the atmosphere and water column. Inventory is a useful measure to trace the distribution and transport of radionuclides in the sediments.

The inventories are calculated from activities (mBq/g) of the pertinent radionuclide in sediment cores, using the Eq. (8):

$$I = \sum(\rho_i \cdot A_i \cdot z_i) \quad (9)$$

where: I=inventory of radionuclide (mBq/cm^2); ρ_i= dry bulk density (g dry sediment/cm^3 wet sediment) of the i-th depth interval; A_i=activity (mBq/g) of the i-th depth interval; and z_i=thickness of i-th depth interval (cm).

In steady-state, supply of radionuclides will be balanced by the removal by radioactive decay. Therefore, fluxes are related to the sediment inventories by:

$$F = \lambda \cdot I \quad (10)$$

where: F=flux of radionuclide (mBq/cm^2 yr); l=decay constant (yr^{-1}); I=inventory of the radionuclide (mBq/cm^2).

Table 7. Inventories and fluxes of ^{7}Be, $^{234}Th_{xs}$ and $^{210}Pb_{xs}$ in Ulleung Basin of the East Sea.

Station No.	Inventory (mBq/cm^2)			Flux (mBq/cm^2 · yr)			Reference
	^{7}Be	$^{234}Th_{xs}$	$^{210}Pb_{xs}$	^{7}Be	$^{234}Th_{xs}$	$^{210}Pb_{xs}$	
A17-1	305	334	2856	1448	3503	89	This study
A18-1	504	824	4277	2392	3913	133	"
A19	371	866	2549	1760	4108	79	"
East Sea			461–2083			14–65	Moon, 1999
East Sea			1022–3817			32–118	Hong et al., 1997

Table 8. Comparison of observed mean $^{210}Pb_{xs}$ fluxes with those predicted from water column supply. Predicted $^{210}Pb_{xs}$ flux was calculated from the water column deficit and an atmospheric input.

Station No.	Atmospheric flux* (mBq/cm^2 yr)	Water column deficit† (mBq/cm^2 yr)	Pred. ^{210}Pb Flux (mBq/cm^2 yr)	Obs. ^{210}Pb Flux (mBq/cm^2 yr)	observed/ predicted
A17-1	18.8	43.7	62.5	88.6	1.4
A18-1	18.8	43.7	62.5	132.6	2.1
A19	18.8	43.7	62.5	79.0	1.3

*Flux estimated from soil profiles and 'wet' and 'dry' fall-out of the nuclides at Uljin county located on coastal area of the East Sea. Data from Jung, H. S. (1995); †Data from Moon, D. S. (1999).

Inventories estimated from distribution profiles of radionuclides in sediments were in the range of 305–504 mBq/cm^2 for ^{7}Be, 334–866 mBq/cm^2 for $^{234}Th_{xs}$, and 2549–4277 mBq/cm^2 for $^{210}Pb_{xs}$ (Table 7). Fluxes were in the range of 1448–2392 mBq/cm^2 yr, 3503–4108 mBq/cm^2 yr, and 79–133 mBq/cm^2 yr, respectively (Table 7). We compared the ratios of observed ^{210}Pb flux in sediment to the predicted ^{210}Pb flux (sum of ^{210}Pb fluxes from the atmosphere and water column). The ratios for 3 cores were greater than 1.0, implying additional input of ^{210}Pb due to lateral water movement in this part of Ulleung Basin (Table 8).

CONCLUSIONS

We could clearly resolve sedimentation signals from those of particle mixing by a series of simultaneous measurements of 4 radionuclides (^{7}Be, ^{234}Th, ^{210}Pb, and ^{137}Cs) in 3 cores from the Ulleung Basin of the East Sea. Thus we could pinpoint the sedimentation rates by excluding up to 38% error introduced by the mixing signals. Rates of sedimentation and particle mixing were determined using a one-box advection-diffusion steady-state mixing model. There are four major findings in this study.

1. Estimated sedimentation rates were 0.06–0.08 cm/yr. These values were confirmed by the subsurface maximums of ^{137}Cs activities in the cores.

2. ^{7}Be and ^{234}Th yielded different mixing rates in the same cores. This could be explained by the particle-selective mixing by benthic organisms as in the case of ^{234}Th and ^{210}Pb reported previously (Krishnaswami *et al.*, 1980; Feng *et al.*, 1999). The particle mixing rates were in the range of 0.13–0.65 cm^2/yr.

3. Inventories estimated from distribution profiles of radionuclides in sediments were in the range of 305–504 mBq/cm^2 for ^{7}Be, 334–866 mBq/cm^2 for $^{234}Th_{xs}$ and 2549–4277 mBq/cm^2 for $^{210}Pb_{xs}$. Fluxes were in the range of 1448–2392 mBq/cm^2 yr, 3503–4108 mBq/cm^2 yr, and 79–133 mBq/cm^2 yr, respectively.

4. The reliability of estimated sedimentation rates is improved by the use of multiple tracers in same cores. The use of three tracers with different half-lives prevented us from the probable large errors that we would have encountered otherwise.

ACKNOWLEDGEMENTS

The authors wish to express their thanks to the captain and crew of R/V Tamyang for their technical supports during the cruise. The comments by Dr. J.H. Han (Korea Basic Science Institute) and an anonymous reviewer on the earlier version of the manuscript helped greatly in improving this paper. This study was supported by the Academic Research Fund of the Chungnam National University Research Foundation, 2000.

REFERENCES

Aaboe, E., E.P. Dion and K.K. Turekian, 1981. ^{7}Be in Sargasso Sea and Long Island Sound waters, *J. Geophys. Res.*, **86**:

3255–3257.

Aller, R.C. and D.J. DeMaster, 1984. Estimation of particle flux and reworking at the deep-sea floor using $^{234}Th/^{238}U$ disequilibrium, *Earth and Planetary Science Letters*, **67**: 308–318.

Aller, R.C., Benninger, L.K., and Cochran, J.K., 1980. Tracking particle-associated processes in nearshore environments by use of $^{234}Th/^{238}U$ disequilibrium. *Earth and Planetary Science Letters*, **47**: 161–175.

Aller, R.C. and J.K. Cochran, 1976. The $^{234}Th/^{238}U$ disequilibrium in near-shore sediments: particle reworking and diagenetic time scales, *Earth and Planetary Science Letters*, **29**: 37–50.

Baskaran, M., M. Ravichandran, and T.S. Bianchi, 1997. Cycling of ^{7}Be and ^{210}Pb in a High DOC, Shallow, Turbid Estuary of South-east Texas. *Estuarine, Coastal and Shelf Science*, **45**: 165–176.

Bateman, H., 1910. Solution of a system of differential equations occurring in the theory of radioactive transformations. *Proc. Cambridge Phil. Soc.* **15**: 423.

Casey, W.H., C.R. Olsen, and I.L. Larsen, 1985. The distribution of cosmogenic ^{7}Be in salt marsh soils: Alternatives to particle mixing(abstract), Eos Trans. *AGU*, **66**: 276.

Chough, S.K. 1984. Fine-grained turbidites and associated mass-flow deposits in the Ulleung (Tsusima) Back-arc Basin, East Sea (Sea of Japan). In: Fine-Grained Sediments: Deep-Water Processes and Products, edited by stow, D.A.V. and D.J.W. Piper, *Geol. Soc. London, Spec. Publ.*, **15**: 185–196.

Chough, S.K., K.S. Jeong and E. Honza, 1985. Zoned facies of mass-flow deposits in the Ulleung (Tsusima) Basin, East Sea (Sea of Japan). *Mar.Geol.*, **65**: 113–125.

Cochran, J.K., 1995. Particle mixing rates in sediments of the eastern equatorial Pacific: Evidence from ^{210}Pb, $^{239,240}Pu$ and ^{137}Cs distributions at MANOP sites. *Ceochimica et Cosmochimica Acta*, **49**: 1195–1210.

Cochran, J.K., Hircshberg, D.J., Wang, J. and Dere, C., 1998. Atmospheric Deposition of metal to coastal waters (Long Island sound, New York U.S.A.): Evidence from saltmarsh deposits. *Estuarine, Coastal and Shelf Science*, **46**: 503–522.

Dibb, J.E. and Rice, D.L., 1989. The Geochemistry of Beryllium-7 in Chesapeake Bay. *Eastuarine, Coastal and Shelf Science*, **28**: 379–394.

Dibb, J.E. and Rice, D.L., 1989. Temporal and spatial distribution of Beryllium-7 in the sediments of Chesapeake bay. *Eastuarine, Coastal and Shelf Science*, **28**: 395–400.

DeMaster, D.J. and J.K. Cochran, 1982. Particle mixing rates in deep-sea sediments determined from excess ^{210}Pb and ^{32}Si profiles. *Earth Planet. Sci. Lett.*, **61**: 257–271.

Feng, H., Cochran K.D. and Hirschberg, D.J., 1999. ^{234}Th and ^{7}Be as Tracers for the Sources of Particles to the Turbidity Maximum of the Hudson River Eastuary. *Eastuarine, Coastal and Shelf Science*, **49**: 629–645.

Gerino, M., Aller, R.C., Lee, C., Cochran, J.K., Aller, J.Y., Green, M.A. and Hirsheberg, D., 1998. Comparison of different tracers and methods used to quantify bioturbation during a spring bloom: 234-thorium, luminophores and chlorophyll a. *Estuarine, Coastal and Shelf Science*, **46**: 531–547.

Goldberg, E.D. and Koide, M., 1962. Geochronological studies of deep sea sediments by the ionium/thorium method. *Geochimica et Cosmochimica Aeta*, **26**: 417–450.

Hong, G.H., Kim, S.H., Chung, C.S., Kang, D.J., Shin, D.H., Lee, H.J. and Han, S.J., 1997. ^{210}Pb-derived sediment accumulation rates in the southwestern East Sea (Sea of Japan). *Geo-Marine Letters*, **17**: 126–132.

Hyun, S.M., S.J. Han and J.J. Bahk, 1998. Major element changes in the upper Quaternary sediment of the East Sea (Sea of Japan): their implications for the onset of Holocene. *J. Korean Soc. Oceanogra.*, **33**: 185–184.

Jaakola, T., K. Tolonen, P. Hutunen, and S. Leskinen, 1983. The use of fallout ^{137}Cs and $^{239,240}Pu$ for dating marine and lake sediments. *Hydrobiogia*, **103**: 15–19.

Jaeger, J.M. and C.A. Nittrouer, 1999. Sediment deposition in an Alaskan fjord: controls on the formation and preservation of sedimentary structures in Icy Bay, *Journal of Sedimentary Reserch*, **69**: 1011–1026.

Jung, H.S., 1995, Estimation of atmospheric fluxes of cosmogenic radionuclides ^{7}Be and ^{210}Pb and anthropogenic metals, Masters theis, Chungnam national university, Daejeon, Korea, 52 p.

Kim, K.H and W.C. Burnett, 1983. Gamma-ray spectrometric determination of uranium-series nuclides in marine phosphorites. *Anal. Chem.*, **55**: 1796–1800.

Kim, K.H and W.C. Burnett, 1988. Accumulation and biological mixing of Peru margin sediments. *Mar. Geol.*, **80**: 181–194.

Krishnaswami, S., Benninger, L.K., Aller, R.C. and Von damm, K.L., 1980. Atmospherically-derived radionuclides as tracers of sediment mixing and accumulation in bear-shore marine and lake sediments: evidence from ^{7}Be, ^{210}Pb, and $^{239,240}Pu$. *Earth and Planetary Science Letters*, **47**: 307–318.

Lee, H.J. and Chough, S.K., 1987. Technical note (:bulk density, void ratio, and porosity determined from average grain density and water content): an evaluation of errors. *Marine Geotechnology*, **7**: 53-62.

Miller, K.M. and M. Heit, 1986. A time resolution methodology for assessing the quality of lake sediment cores that are dated by ^{137}Cs. *Limnol. Oceanogr.*, **31**: 1292–1300.

Moon, D.S., 1999. Geochemical Fluxes and Cycling Processes of Uranium Series and Artificial Radionuclides in the East Sea, Ph.D dissertation, Chungnam National Univ., p. 273.

MOST(Ministry of Science and Technology), 1995. A study of Trace Element Composition and Structural Analyses of Geologic and Marine Samples (I), p. 464.

Nittrouer, C.A., Demaster, D.J., Mckee, B.A., Cutshall, N.H. and Larsen, I.L., 1983. The effect of sediment mixing on Pb-210 accumulation rates for the washington continental shelf. *Marine Geology*, **54**: 201–221.

Nozaki, Y., J.K. Cochran, K.K. Turekian and G. Keller, 1977. Radiocarbon and 210Pb distribution in submersible-taken deep-sea cores from project FAMOUS, *Earth Planet. Sci. Lett.*, **34**: 167p.

Manuscript received October 9, 2001
Revision accepted December 12, 2003
Editorial handling: Kyung-Ryul Kim